MYPT1 O-GlcNAcylation controls the sensitivity of fibroblasts to sphingosine-1-phosphate mediated cellular contraction

Nichole J. Pedowitz,[1]* Anna R. Batt,[1]* Narek Darabedian,[1] and Matthew R. Pratt[1,2]

[1]Departments of Chemistry and [2]Biological Sciences, University of Southern California, Los Angeles, CA 90089, United States

Corresponding author: Matthew R. Pratt, matthew.pratt@usc.edu

ABSTRACT

Many intracellular proteins can be modified by N-acetylglucosamine, a posttranslational modification known as O-GlcNAc. Because this modification is found on serine and threonine side-chains, O-GlcNAc has the potential to dynamically regulate cellular signaling pathways through interplay with phosphorylation. Here, we discover and characterize one such pathway. First, we find that O-GlcNAcylation levels control the sensitivity of fibroblasts to actin contraction induced by the signaling lipid sphingosine-1-phosphate (S1P). In subsequent mechanistic investigations, we find that S1P agonizes the S1PR2 receptor, resulting in activation of the Rho/Rho kinase signaling pathway. This pathway typically culminates in the phosphorylation of myosin light chain (MLC), resulting in myosin activation and cellular contraction. We find that O-GlcNAcylation of the phosphatase subunit MYPT1 inhibits this pathway by blocking MYPT1 phosphorylation, maintaining its activity and causing the dephosphorylation of MLC. Therefore, MYTP1 O-GlcNAcylation levels function as a rheostat to regulate the sensitivity of cells to S1P-mediated cellular contraction. Our findings have important implications for the role of in fibroblast motility and differentiation, as well as several other signaling pathways that use MLC/MYTP1 to control actin contraction in various tissues.

INTRODUCTION

O-GlcNAcylation is a form of protein glycosylation that is uniquely suited to regulate cellular signaling pathways (Figure 1a). This intracellular posttranslational modification involves the transfer of the monosaccharide *N*-acetylglucosamine to serine and threonine side chains of proteins throughout the cytosol, nucleus, and mitochondria of all animals cells[1-3]. Unlike most forms of cell surface glycosylation, this core GlcNAc moiety is not further elaborated by additional carbohydrates and is dynamically regulated through the action of two enzymes. O-GlcNAc transferase (OGT) uses the donor sugar UDP-GlcNAc to install O-GlcNAc onto substrates, while O-GlcNAcase (OGA) removes them[4-6], setting up a scenario potentially similar to the cycling of protein phosphorylation. Additionally, the amounts of O-GlcNAcylation have been shown to change upon alterations in cellular environment through the sensing of different biologically inputs. For example, increase flux of glucose into the cell results in the biosynthesis of more UDP-GlcNAc and a corresponding dynamic increase in overall O-GlcNAcylation levels. Additionally, a wide-range of cellular stressors also result in relatively short-lived increases in the amounts of O-GlcNAc that play a phenotypically protective role. Therefore, it is not necessarily surprising that the human diseases of diabetes and cancer uniformly display elevated O-GlcNAcylation in comparison to healthy individuals or tissues,

respectively. In contrast, O-GlcNAcylation levels have been observed to be lower in the brains of Alzheimer's disease patients, and genetic loss of OGT in mouse neurons results degeneration. Taken together, these general observations indicate that O-GlcNAc should modulate various proteins and pathways and that disregulation of these events contributes to human disease. An attractive hypothesis in the O-GlcNAc field has been a direct relationship between the O-GlcNAc modification and phosphorylation of proteins (Figure 1b) [7]. For example, O-GlcNAcylation of the kinase Akt at Thr305 and Thr312 prevents phosphorylation at nearby Thr308 and impairs Akt signaling[8]. Similarly, O-GlcNAc modification of casein kinase II (CK2) at Ser347 antagonizes phosphorylation at nearby Thr344, thereby reducing the stability and activity of this kinase[9]. In contrast, activating phosphorylation of the transcription factor cyclic AMP-response element binding protein (CREB) at Ser133 is required for subsequent O-GlcNAcylation at Ser40, which can then repress its transcriptional activity with key consequences for memory formation[10]. However, despite these and some other examples, and the theoretical attractiveness of O-GlcNAc as a regulator of cell signaling, the cases where we understand molecularly how this modification controls specific cascades remains limited.

One reason for our narrow understanding of O-GlcNAc has been an absence of applicable biological tools. Genetic ablation of either OGT or OGA is lethal during development in most model organisms and loss of OGT results in mammalian cell death in culture[11,12]. Additionally, while antibodies against O-GlcNAc are available they do not detect all modifications nor can be readily used to determine absolute O-GlcNAcylation stoichiometry. Fortunately, a range of chemical tools have been developed over the past decade that overcome these limitations, including small molecule inhibitors of both OGT and OGA that enable the dynamic control of overall O-GlcNAcylation levels and chemoenzymatic labeling techniques for the identification and characterization of protein substrates. Here, we apply these chemical tools to investigate our serendipitous discovery linking the signaling lipid sphingosine-1-phosphate (S1P) to actin cytoskeletal remodeling through the O-GlcNAc modification status of the phosphatase regulatory subunit MYPT1.

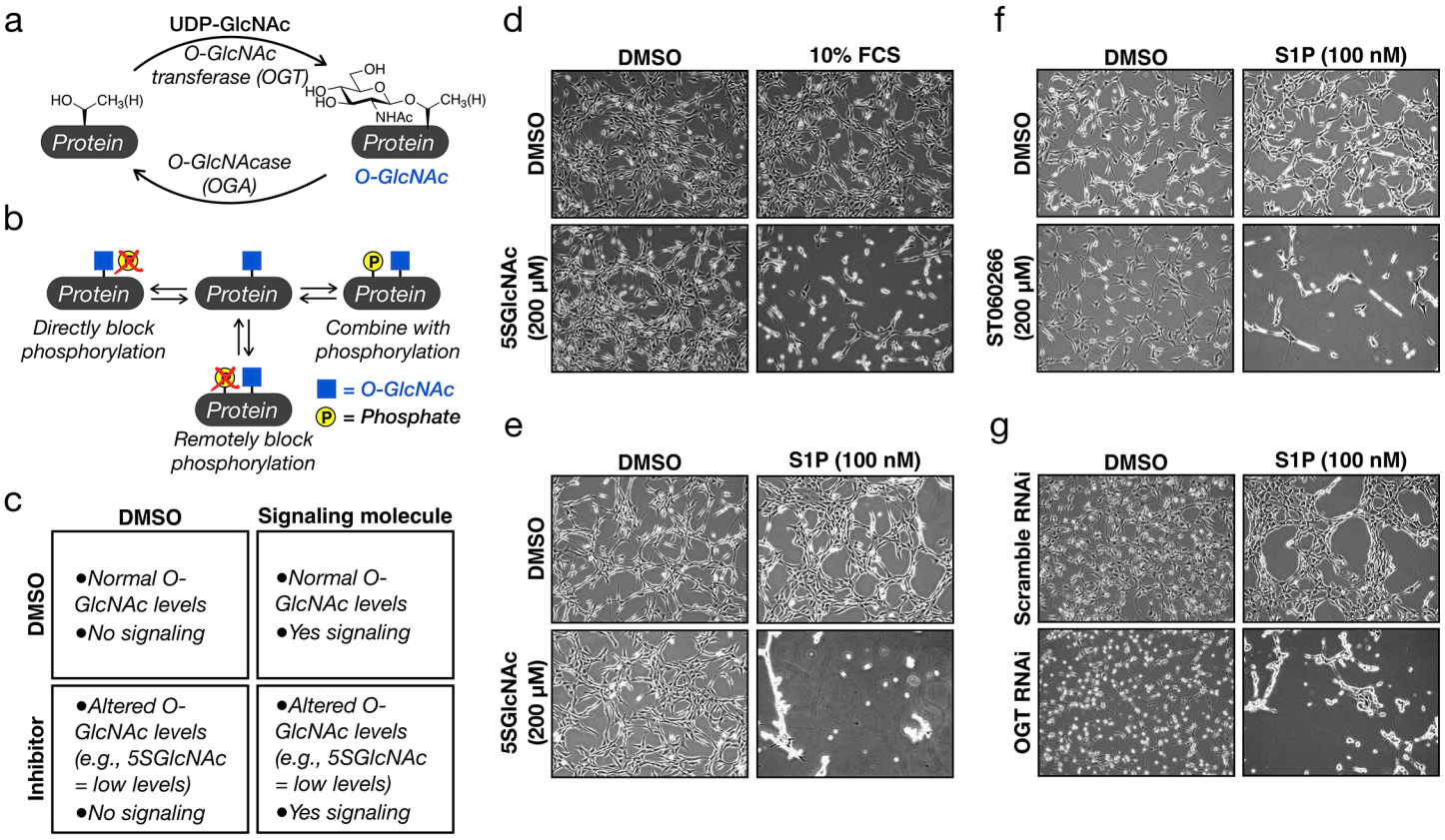

Figure 1. O-GlcNAc controls the sensitivity of fibroblasts to sphingosine-1-phosphate (S1P) mediated cell contraction. a) O-GlcNAcylation is the dynamic addition to N-acetylglucosamine to serine and threonine residues of intracellular proteins. b) O-GlcNAcylation has its own functions but can also antagonize phosphorylation, both directly and remotely, as well as combine with phosphorylation to illicit biological outcomes. c) Schematic layout of our general experimental conditions. d) NIH3T3 cells were treated with either DMSO or the OGT inhibitor 5SGlcNAc (200 µM) for 16 h before addition of either more DMSO or 10% FCS for 30 min. The contraction phenotype was then visualized using bright-field microscopy. e) NIH3T3 cells were treated with either DMSO or 5SGlcNAc (200 µM) for 16 h before addition of either more DMSO or S1P (100 nM) for 30 min. The contraction phenotype was then visualized using bright-field microscopy. f) NIH3T3 cells were treated with either DMSO or the OGT inhibitor ST060266 (200 µM) for 16 h before addition of either more DMSO or S1P (100 nM) for 30 min. The contraction phenotype was then visualized using bright-field microscopy. g) NIH3T3 cells were transfected with either scramble or OGT-targeted RNAi for 48 h before addition of either more DMSO or S1P (100 nM) for 30 min. The contraction phenotype was then visualized using bright-field microscopy.

RESULTS

O-GlcNAcylation controls fibroblast contraction in response to the serum lipid sphingosine-1-phosphate. During the course of our previous investigation into the roles of O-GlcNAcylation in apoptosis, we encountered a dramatic phenotypic change in NIH3T3 fibroblasts upon reduction of overall O-GlcNAcylation levels followed by treatment with fetal calf serum (FCS). As schematized in Figure 1c, these fibroblasts were treated with the OGT inhibitor 5SGlcNAc (200 µM) for 16 h to give a downregulation of global O-GlcNAcylation (Supplementary Figure 1a). Upon subsequent addition of 10% FCS, the cells underwent a rapid (10 - 30 min) morphological change, resulting in their contraction and detachment from the culture

plate (Figure 1d and Supplementary Video 1). Intrigued by this result, we then screened multiple protein factors, cytokines, and lipids commonly found in serum. Strikingly, we only detected this phenotype upon S1P treatment (100 nM) and not with any of the other serum components (Figure 1e, Supplementary Figure 1e and Supplementary Video 2), indicating that cellular signaling initiated by this lipid is responsible for our observation. In order to confirm that this phenotype is indeed due to a reduction in O-GlcNAcylation and not a potential off-target effect of 5SGlcNAc, we next treated fibroblasts with either an orthogonal OGT inhibitor (ST060266, 200 μM) or RNAi directed again OGT (Supplementary Figure 1b & c). In both cases, we found an identical morphological change upon addition of S1P (Figures 1f & g), confirming the O-GlcNAc dependence of the phenotype.

Next, we set out to determine whether this signaling pathway was only operative under low O-GlcNAcylation levels or if the fibroblasts were simply sensitized to S1P-mediated signaling under these conditions. Accordingly, we again treated NIH3T3 cells with either DMSO vehicle or 5SGlcNAc (200 μM) for 16 h followed by a range of S1P concentrations from 0.05 to 5 μM. Consistent with the second model, fibroblasts with "normal" and reduced O-GlcNAcylation levels both underwent contraction at the higher concentrations of S1P, but cells treated with the OGT inhibitor displayed increased sensitivity to lower S1P amounts (Figure 2a). We then quantified the amounts of cellular contraction by measuring the surface area occupied by the cells and found the difference in contraction to be statistically significant (Figure 2b). Importantly, this increased sensitivity was observed in multiple biological replicates (Supplementary Figures 2a & b). Given that NIH3T3 cells with baseline O-GlcNAcylation will respond to higher concentrations of S1P, we next asked whether raising the modification levels would decrease their sensitivity to the signaling lipid. Accordingly, we treated these fibroblasts with either DMSO vehicle or the OGA inhibitor Thiamet-G (10 μM), resulting in increased overall O-GlcNAcylation (Supplementary Figure 1a). Gratifyingly, we found the Thiamet-G treated cells to be significantly more resistant to S1P concentrations compared to the control (Figures 2c & d), and again this phenotypic difference was recapitulated in multiple biological replicates (Supplementary Figures 2c & d). As mentioned in the introduction, O-GlcNAcylation levels are responsive to changes in extracellular glucose concentrations, raising the possibility that the modification could act as a nutrient sensor to control S1P-dependent signaling. To test this possibility, we cultured NIH3T3 cells in media containing either 1 or 9 g L^{-1} glucose for 48 h, resulting in the expected differences in O-GlcNAcylation levels (Supplementary Figure 1d). As predicted, we found that the cells cultured in low glucose were indeed more sensitive to S1P-mediated contraction compared to those grown in high glucose (Figures 2e & f and Supplementary Figures 2e & f). Together these results indicate that O-GlcNAcylation acts as a molecular buffer to control an S1P signaling pathway that culminates in fibroblast contraction and detachment.

The S1P-mediated contraction phenotype results from signaling through one of five S1P G-protein coupled receptors (S1PR2). S1P is an endogenous signaling lipid[13-19] produced intracellularly from the phosphorylation of ceramide by sphingosine kinases 1 and 2 (SphK1, SphK2). It can then be transported outside of the cell and signal through a family of

five G-protein coupled receptors (GPCRs) (S1PR1 through S1PR5, Figure 3a). Subsequent coupling of these GPCRs to different classes of G-proteins results in the activation of several associated downstream signaling pathways (Figure 3a) [20-22] S1P plays roles in many biological events, including cell survival, proliferation, motility, and adherence. Therefore, it is not surprising that it has been shown to contribute to diverse areas of human health and disease, such as cardiovascular development and control of blood pressure, regulation of immune cell migration, and fibrosis and wound healing.

As a next step towards discovering the molecular mechanism by which O-GlcNAc regulates S1P signaling, we first used RT-PCR to determine which of the S1PRs were actively transcribed in our fibroblasts. We found that all five receptors had the potential to be expressed in this cell line (Supplementary Figure 3a). Given that this approach was unable to narrow down the potential S1PR responsible, we then turned to small molecule pharmacology. Specifically, we first treated NIH3T3 cells with either DMSO or 5SGlcNAc (200 μM) to modulate O-GlcNAcylation levels as above. We then added individual selective antagonists of S1PR1 through S1PR4 (1 μM) for 10 min immediately followed by S1P (100 nM). Visualization of the cellular contraction phenotype demonstrated that only blockage of S1PR2 signaling could prevent the S1P-mediated morphological change (Figure 3b and Supplementary Figures 3b & c), indicating that the other three receptors (S1PR1, R3, and R4) are not involved. Unfortunately, S1PR5 does not yet have a selective antagonist, and therefore we could not rule it out with these data. However, when we treated NIH3T3 cells with a selective agonist of this receptor, we observed no phenotypic change regardless of O-GlcNAcylation levels (Supplementary Figures 3d & e). Finally, to test whether S1PR2 agonism alone is sufficient to activate the pathway, we exposed DMSO- or 5SGlcNAc-treated cells to different concentrations of a selective S1PR2 agonist. Notably, we found that low concentrations of this agonist (1 μM) resulted in cell contraction under low O-GlcNAcylation levels while a higher concentration (5 μM) induced the phenotype universally (Figure 3c and Supplementary Figures 3f & g), similar to what we observed for different concentrations of S1P. Together these results demonstrate that O-GlcNAcylation controls a signaling pathway that is likely downstream of S1PR2.

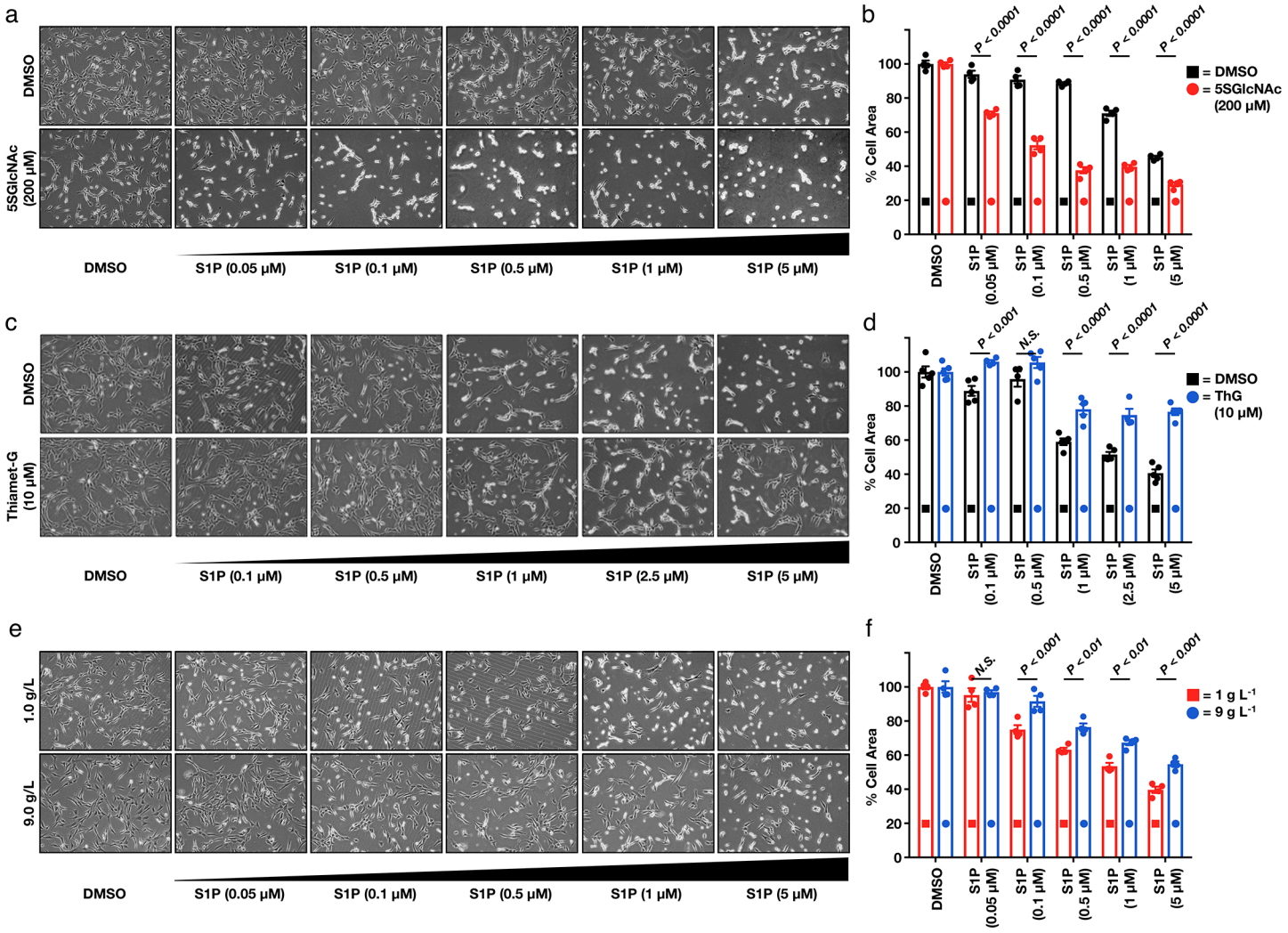

Figure 2. O-GlcNAc acts as a S1P-signaling rheostat. a) Lowering O-GlcNAcylation levels increases the sensitivity of NIH3T3 cells to S1P induced cell contraction. NIH3T3 cells that had been treated with either DMSO or 5SGlcNAc (200 µM) for 16 h before addition of the indicated concentrations of S1P for 30 min. The contraction phenotype was then visualized using bright-field microscopy. b) Quantitation of the data in (a). Results are the mean ± SEM of the relative culture plate area taken-up by cells in four randomly selected frames. Statistical significance was determined using a 2-way ANOVA test followed by Sidak's multiple comparisons test. c) Raising O-GlcNAcylation levels decreases the sensitivity of NIH3T3 cells to S1P induced cell contraction. NIH3T3 cells that had been treated with either DMSO or the OGA inhibitor Thiamet-G (10 µM) for 20 h before addition of the indicated concentrations of S1P for 30 min. The contraction phenotype was then visualized using bright-field microscopy. d) Quantitation of the data in (c). Results are the mean ± SEM of the relative culture plate area taken-up by cells in four randomly selected frames. Statistical significance was determined using a 2-way ANOVA test followed by Sidak's multiple comparisons test. e) Glucose concentration controls the sensitivity of NIH3T3 cells to S1P induced cell contraction. NIH3T3 cells were cultured in the indicated amounts of glucose for 48 h before addition of the indicated concentrations of S1P for 30 min. The contraction phenotype was then visualized using bright-field microscopy. f) Quantitation of the data in (e). Results are the mean ± SEM of the relative culture plate area taken-up by cells in four randomly selected frames. Statistical significance was determined using a 2-way ANOVA test followed by Sidak's multiple comparisons test.

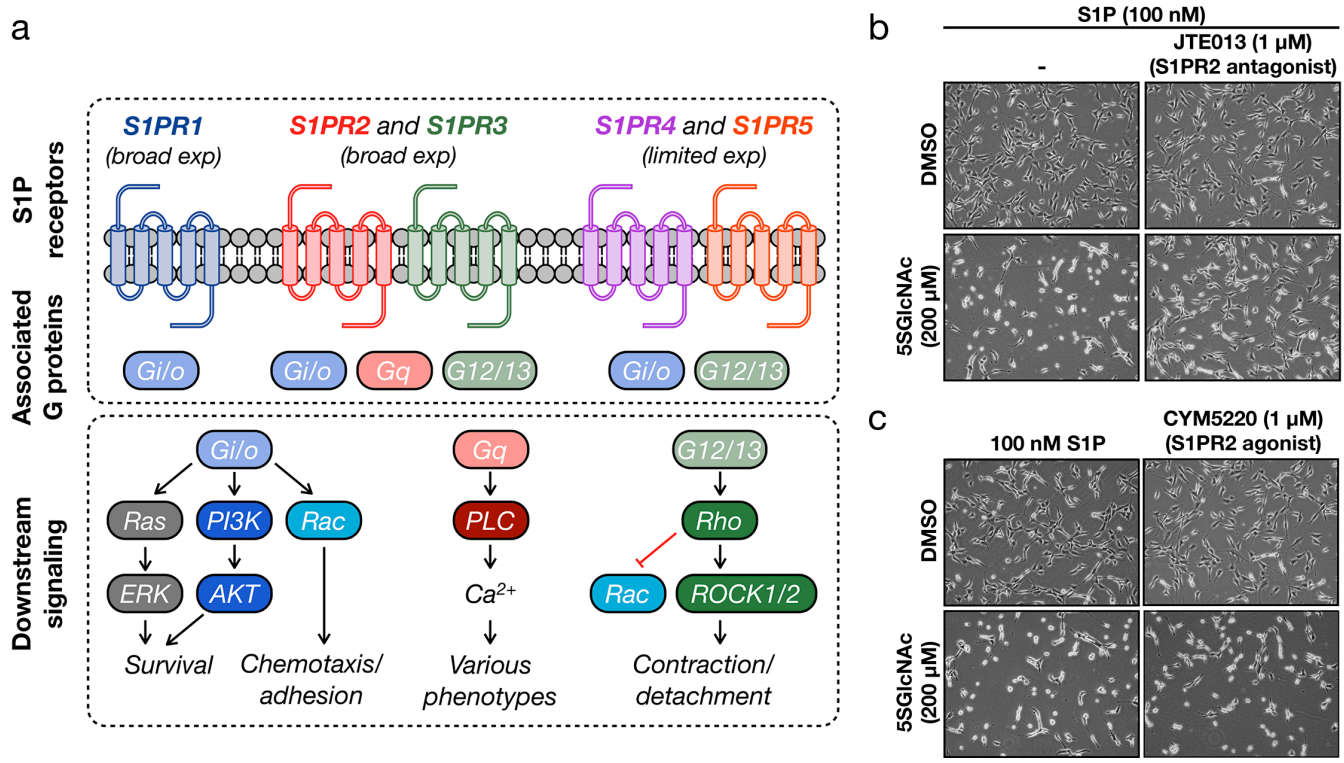

Figure 3. Signaling through the second S1P receptor, S1PR2, is responsible for the contraction phenotype. a) Schematic of the major S1P signaling pathways in mammalian cells. S1P can agonize five different GPCRs (S1PR1 to R5) resulting in the potential activation of various downstream signaling pathways. b) Antagonizing S1PR2 blocks S1P-mediated contraction. NIH3T3 cells were treated with either DMSO or 5SGlcNAc (200 μM) for 16 h. The same cells were then treated with either additional DMSO or the S1PR2-selective antagonist JTE013 (1 μM) for 10 min followed by S1P (100 nM) for 30 min. The contraction phenotype was then visualized using bright-field microscopy. c) S1PR2-selective agonism is sufficient to induce S1P mediated contraction. NIH3T3 cells were treated with either DMSO or 5SGlcNAc (200 μM) for 16 h. The same cells were then treated with either S1P (100 nM) or the S1PR2-selective agonist CYM5220 (1 μM) for 30 min. The contraction phenotype was then visualized using bright-field microscopy.

O-GlcNAc controls signaling through Rho and Rho kinase (ROCK) to regulate the activation status of myosin light chain (MLC) and its associated phosphatase MYPT1. Because of the nature of the observed phenotype, we decided to focus on the established role of S1P signaling in the regulation of cell adhesion and motility through Rho GTPase (Figure 3a). Briefly, S1PR agonism can active Rho in turn increasing the catalytic activity of two isoforms of Rho kinase, termed ROCK1/2[23], ultimately resulting in actin contraction (Figure 4a) [21,24-26]. More specifically, activated ROCK1/2 will phosphorylate myosin light chain (MLC) at two serines (Thr18 & Ser19) resulting in the formation of an active myosin complex and actin filament contraction[26-28]. To avoid unwanted activation of this pathway, cells are equipped with molecular brakes in the form of the phosphatase regulatory subunit MYPT1 that mediates the dephosphorylation MLC. Previous work has shown that ROCK1/2 can also phosphorylate MYTP1 at Thr696 and Thr853[29-32]. This results in the deactivation of MYPT1[33], effectively cutting the breaks on the pathway and ensuring myosin activation.

To test whether ROCK1/2 activity was indeed required for our observed contraction phenotype, we again treated NIH3T3 cells with either DMSO or 5SGlcNAc (200 μM) for 16 h, followed by the ROCK1/2 inhibitor Y27632 (10 μM) for an additional hour before addition of S1P (0.05 - 5 μM). Notably, we observed no contraction of any cells at all concentrations of S1P (Supplementary Figure S4). With result confirming the importance of ROCK1/2, we moved on to explore the phosphorylation status of its downstream targets MLC[34] and MYPT1[35,36]. In order to confirm previously published results, we first treated NIH3T3 cells with normal O-GlcNAcylation levels to a high concentration of S1P (5 μM) that results in their contraction. After different lengths of time, we collected the cells and subjected the corresponding lysates to analysis by Western blotting (Figure 4b). As expected, we observed increasing phosphorylation of MLC at Ser18/Thr19 that peaked approximately 10 min after S1P addition and corresponded well with the overall timing of cell contraction. Next, we performed a similar analysis of NIH3T3 cells that had been pre-treated with either DMSO or 5SGlcNAc (200 μM) for 16 h before addition of a low concentration of S1P (100 nM) (Figure 4c). In cells treated with DMSO and thus having normal O-GlcNAcylation levels, we found no detectable increase in MLC or MYTP1 phosphorylation. However, in cells with depleted O-GlcNAc (i.e., 5SGlcNAc treated), we detected a rapid increase in phosphorylation of both MLC and MYPT1. Importantly, the oscillation of phosphorylation on MYTP1 that we see is consistent with previous reports and relates to the function of MYTP1 as its own phosphatase and therefore a biological timer of this signaling pathway in response to compressive force[37].

MYPT1 is a heavily and dynamically O-GlcNAcylated protein. We next set out to identify which protein in the Rho/ROCK signaling pathway was potentially regulated by O-GlcNAc. We chose to focus on MLC and MYPT1 first, as they were both some of the earliest proteins to be identified as O-GlcNAcylated[38,39]. In order to ascertain the O-GlcNAcylation status of these proteins, we took advantage the chemoenzymatic labeling protocol originally developed by the Hsieh-Wilson and Qasba labs (Figure 5a) [40,41]. Briefly, we first used this method to install a cleavable biotin tag onto all endogenous O-GlcNAc modifications in NIH3T3 cell lysates. After incubation with streptavidin beads and extensive washing, the O-GlcNAcylated proteins were eluted and analyzed by Western blotting. In accordance with previous reports, we identified both MLC and MYPT1 to be O-GlcNAcylated (Figure 5b). The known O-GlcNAcylated protein nucleoporin 62 (Nup62) served as a positive control with β-actin as a negative control in this experiment. Notably, while both MLC and MYPT1 are indeed O-GlcNAcylated, when we normalized the amount of input to our O-GlcNAc pulldown, we found that MYPT1 was modified at dramatically higher levels compared to MLC and similar to the constitutively O-GlcNAcylated Nup62 (Figure 5c). Therefore, we chose to move forward with MYPT1 as the most likely candidate to be regulated in the pathway.

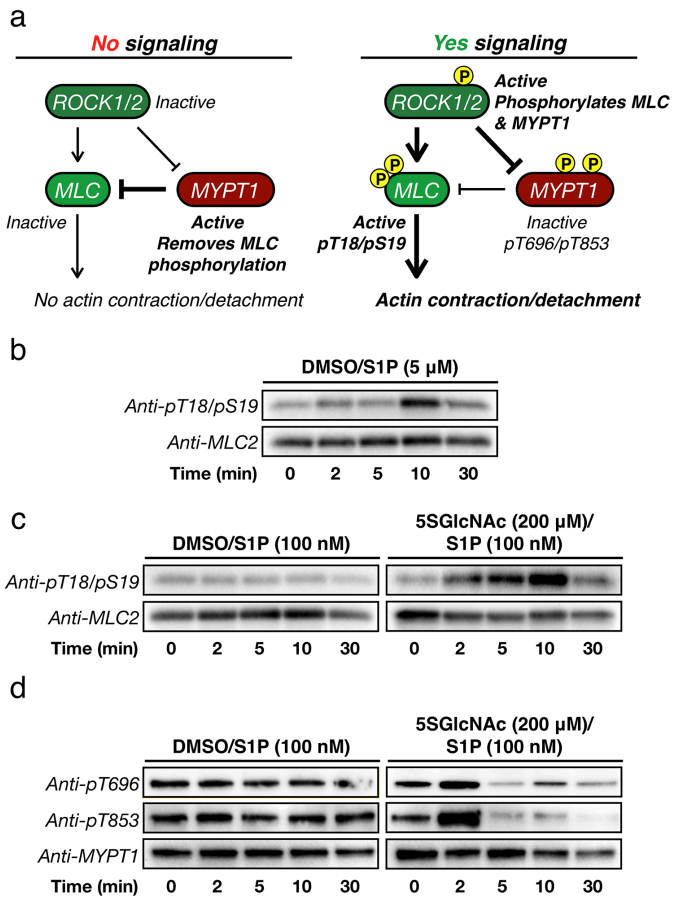

Figure 4. O-GlcNAcylation levels control S1P-mediated phosphorylation of MLC and MYPT1. a) Schematic of the ROCK-signaling pathway that can result in cellular contraction. Under no or low signaling conditions ROCK does not phosphorylated MLC or MYPT1 and MYPT1 remains active to dephosphorylate MLC. Upon induction of signaling ROCK phosphorylates both MLC to activate contraction and MYPT1 to inactivate dephosphorylation, effectively pushing on the gas and cutting the brake. b) MLC is phosphorylated under high S1P signaling. NIH3T3 cells were treated with S1P (5 μM) for the indicated lengths of time. MLC phosphorylation, and thus activation, was visualized using Western blotting. c) MLC is phosphorylated under low S1P signaling when O-GlcNAc levels are reduced. NIH3T3 cells were treated with either DMSO or 5SGlcNAc (200 μM) for 16 h followed by S1P (100 nM) for the indicated lengths of time. MLC phosphorylation, and thus its activation, was visualized using Western blotting. d) MYPT1 is phosphorylated under low S1P signaling when O-GlcNAc levels are reduced. NIH3T3 cells were treated with either DMSO or 5SGlcNAc (200 μM) for 16 h followed by S1P (100 nM) for the indicated lengths of time. MYPT1 phosphorylation, and thus its deactivation, was visualized using Western blotting.

Consistent with the high levels of modification we observed in our pulldown, recent proteomics experiments using the same chemoenzymatic strategy have identified many different endogenous MYPT1 O-GlcNAcylation sites[42-44] localized around two different regions of the protein (Figure 5d). The most N-terminal of these areas, with modification at Ser379 and Thr381, is located near the portion of MYPT1 responsible for binding the phosphatase catalytic subunit PP1cδ and its substrate, phosphorylated MLC[45-47]. The second region contains nine identified O-GlcNAcylation sites (Ser566, Thr570, Thr577, Ser585, Ser589, Thr590, Thr592 & Thr594) clustered within a serine/threonine rich region, as well as tenth site slightly more distant at Thr637. These modification sites are located nearer to the inhibitory phosphorylation sites, and the portions

of MYPT1 responsible for interacting with ROCK1/2 and the myosin motor complex[32,45-47]. Despite the clear potential for MYTP1 to be heavily O-GlcNAcylated, the exact stoichiometry of endogenous modification had not been previously measured to our knowledge. To accomplish this, we again took advantage of the chemoenzymatic methodology (Figure 5a), but instead of installing an enrichment tag, we modified each O-GlcNAc moiety with a polyethylene glycol (PEG) chain of either 2 or 5 kDa in molecular weight. This mass-shifting approach causes the O-GlcNAcylated fraction of a protein to run higher on an SDS-PAGE gel for subsequent analysis by Western blotting[48,49]. We applied this technique to NIH3T3 cells under three sets of conditions: 5SGlcNAc treatment (200 μM) to lower O-GlcNAcylation levels, DMSO vehicle to leave them unchanged, or Thiamet-G treatment (10 μM) to raise them. We then visualized endogenous MYTP1 by Western blotting (Figure 5e). Under basal O-GlcNAcylation levels (i.e., DMSO treatment), we found that MYTP1 is indeed highly modified with essentially 100% of the protein running at mass-shifted molecular weights, and these modifications are largely removed upon treatment with 5SGlcNAc. With Thiamet-G treatment, we observed some potential further upward shift of the MYPT1 bands, suggesting an increase in O-GlcNAcylation levels. However, the most obvious change was an overall decrease in our ability to detect MYTP1. We believe that this is due to the reduced affinity of some antibodies to highly PEGylated proteins, which we previously found for Nup62[49]. In an attempt to overcome this issue, we next generated NIH3T3 cells that stably express a FLAG-tagged version of MYPT1 (Supplementary Figure 5) and performed the same mass-shifting analysis with an anti-FLAG antibody (Figure 5f). Again, we saw near total O-GlcNAcylation of MYPT1 at multiple sites, and we confirmed that the modification stoichiometry could be dialed down or up upon 5SGlcNAc or Thiamet-G treatment, respectively. Unfortunately, we still detected some loss of anti-FLAG signal upon Thiamet-G treatment and the correspondingly high O-GlcNAcylation levels. Therefore, we next used an anti-FLAG immunoprecipitation (IP) to enrich MYPT1. We then observed the relative O-GlcNAcylation levels using an anti-O-GlcNAc antibody and confirmed that the protein's modification status can be both down- and upregulated by inhibitor treatment (Figure 5g). Finally, we used both mass-shifting and anti-FLAG IP to demonstrate that MYTP1 O-GlcNAcylation levels will change in response to alterations in glucose concentration (1 vs. 9 g L^{-1}) in the media (Figures 5h & i). Notably, these glucose-responsive differences in O-GlcNAcylation were smaller than those created by inhibitor treatment, in agreement with their more subtle effect on the cellular contraction phenotype (Figure 2).

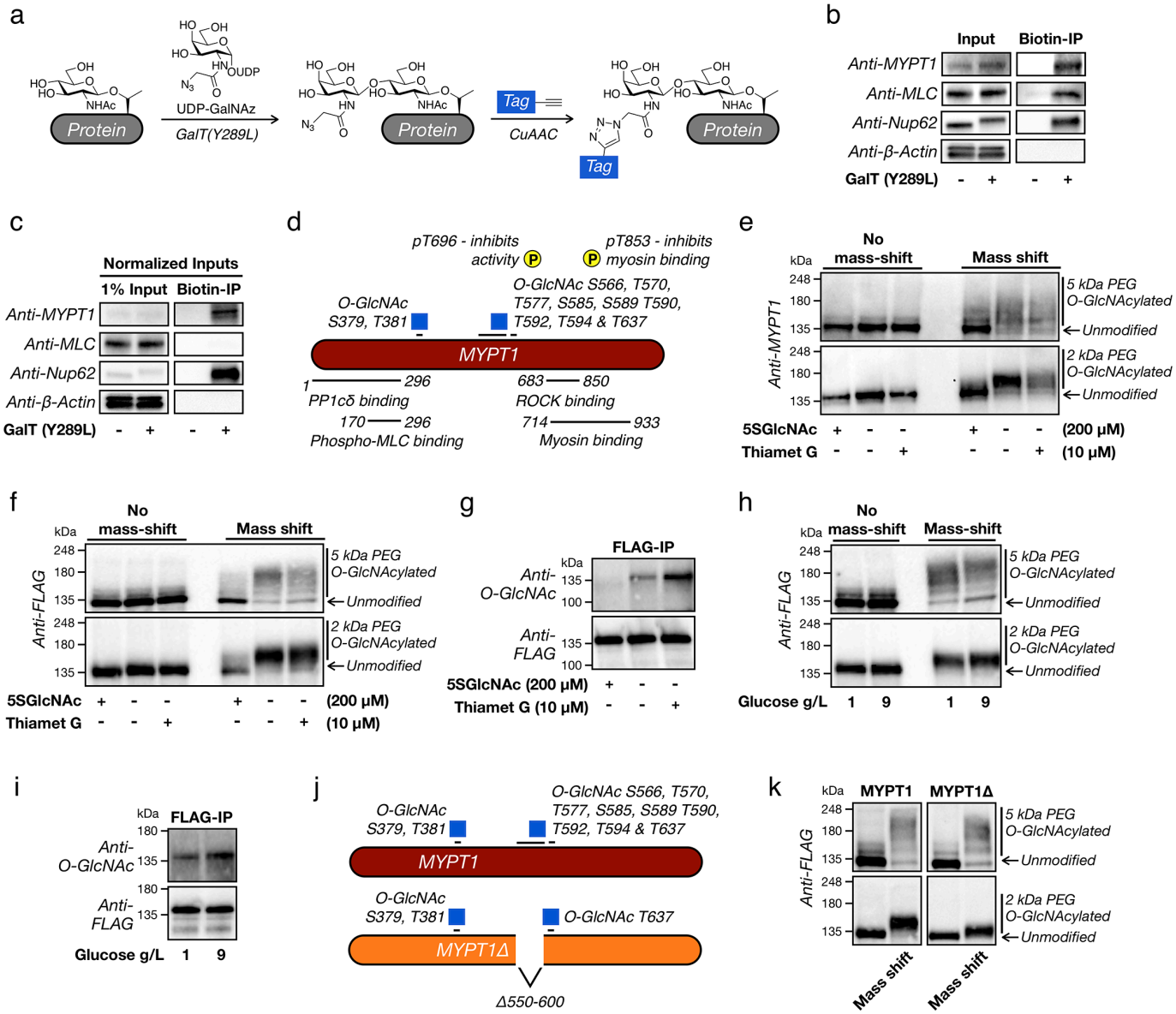

Figure 5. MYPT1 is heavily and dynamically O-GlcNAc modified near its ROCK-binding domain. a) The chemoenzymatic method for detecting O-GlcNAc modifications. Endogenous O-GlcNAc moieties are enzymatically modified with an azide-containing sugar that can then be used for the subsequent installation of tags using bioorthogonal chemistry. b) MLC and MYPT1 are both O-GlcNAcylated. O-GlcNAcylated proteins from NIH3T3 cells were enriched using chemoenzymatic labelling and analyzed by Western blotting. Nucleoporin 62 (Nup62) is a known, heavily O-GlcNAcylated protein, and β-actin serves as a negative control. c) MYPT1 is highly O-GlcNAcylated, while MLC is not. the samples in (b) were normalized for inputs and analyzed by Western blotting. d) Schematic of identified MYPT1 O-GlcNAcylation sites, as well as the two deactivating phosphorylation sites and regions of MYPT1 responsible for critical protein-protein interactions. e) Endogenous MYPT1 is heavily and dynamically O-GlcNAcylated. NIH3T3 cells were treated with either 5SGlcNAc (200 μM), Thiamet-G (10 μM), or DMSO vehicle for 16, 20, or 20 h respectively. The O-GlcNAcylated proteins were then subjected to chemoenzymatic modification and then "mass-shifted" by PEGylation causing the modified fraction of proteins to run at higher molecular weights when analyzed by Western blotting. f-i) NIH3T3 cells stably expressing FLAG-tagged MYTP1 were treated under the indicated conditions before analysis by either mass-shifting or IP-Western blot. j) Schematic of the MYPT1Δ protein, which lacks the major O-GlcNAcylated region of the protein. k) MYPT1Δ loses a notable amount of O-GlcNAcylation. The O-GlcNAcylation levels of FLAG-tagged MYPT1 or MYPT1Δ were analyzed using mass-shifting.

O-GlcNAcylation of the MYTP1 serine/threonine rich region inhibits its phosphorylation and controls the sensitivity of cells to S1P-mediated contraction signaling. Previous experiments aimed at characterizing the MYPT1/ROCK interaction using recombinant proteins demonstrated that the serine/threonine region slightly inhibited this binding event. Therefore, we hypothesized that O-GlcNAcylation in this location would increase this inhibition and prevent MYPT1 phosphorylation and therefore inactivation. To test this possibility, we first generated NIH3T3 cells that stably express a version of MYTP1 where the serine/threonine rich region (residues 550-600) was deleted, termed MYPT1Δ (Figure 5j). Importantly, MYTP1Δ displayed essentially identical expression when compared to stably expressed MYTP1 (Supplementary Figure 5). We then used the mass-shifting assay to examine the O-GlcNAcylation stoichiometry of these proteins and found the levels of MYTP1Δ modification noticeably reduced (Figure 5k), consistent with the localization of a reasonable fraction of O-GlcNAc to this region.

In order to generate these cells, we used human MYPT1, which is 93% identical to the mouse protein and enabled us to use RNA interference to selectively knockdown the endogenous MYPT1 in NIH3T3 cells (Supplementary Figure 6a & b). We then subjected these cells to the same range of S1P concentrations (0.05 - 5 μM) as above and measured the relative amounts of cell contraction (Figure 6a & b). As evidence for the important role of this region, we found that MYPT1Δ expressing cells were significantly more sensitive to S1P-mediated contraction signaling. Again, this phenotype was observed in multiple biological replicates (Supplementary Figure 7). To more directly test this model, we visualized the phosphorylation status of both MLC and MYPT1(Δ) after different lengths of treatment time with a low concentration of S1P (100 nM) (Figure 6c). As predicted, we observed dramatically less phosphorylation of both proteins in the cells expressing MYPT1 versus those expressing MYPT1Δ. These results are consistent with a model where O-GlcNAcylation in the serine/threonine region prevents MYPT1 phosphorylation at low concentrations of S1P and this regulatory system is lost in the MYTP1Δ mutant (Figure 6d).

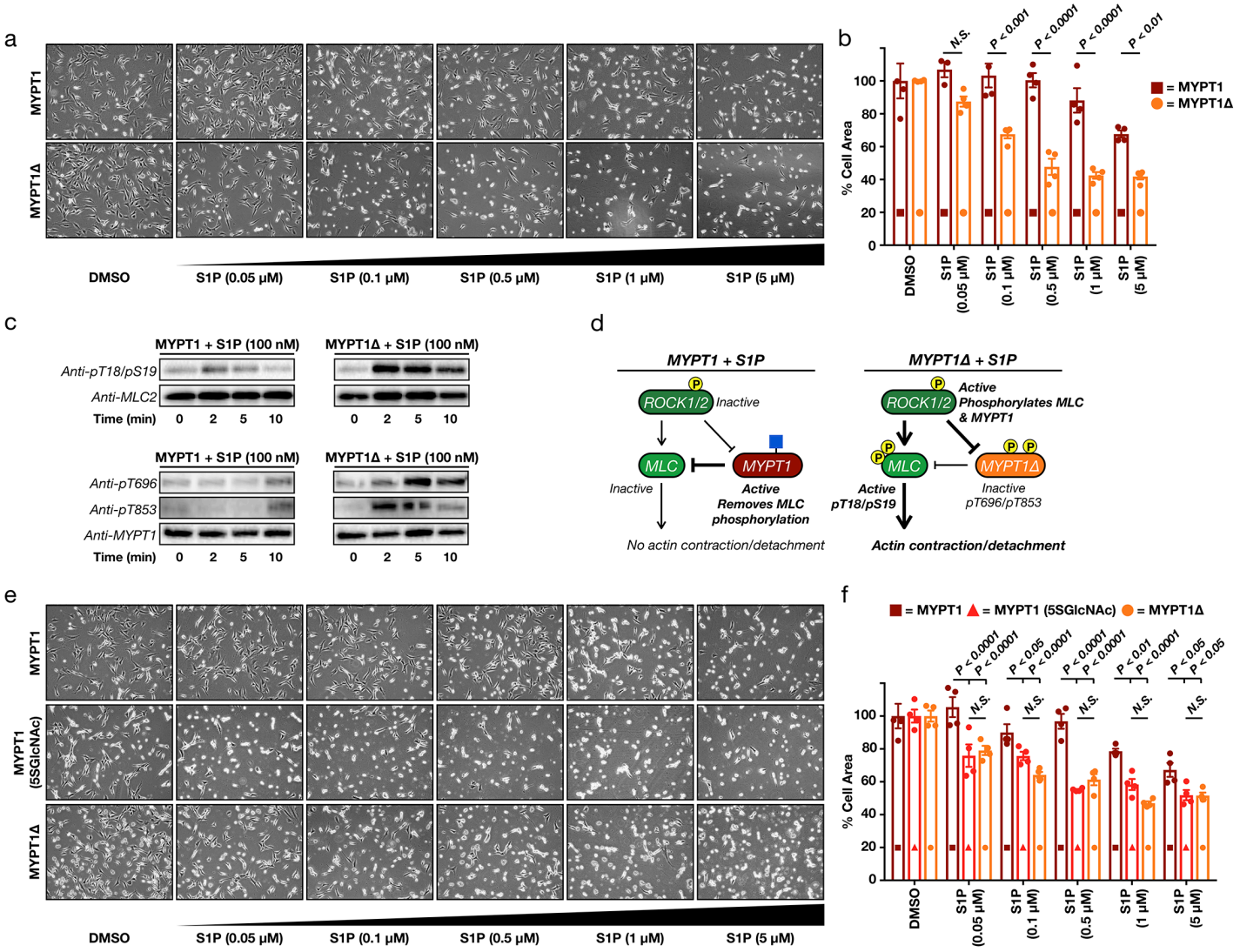

Figure 6. MYPT1 O-GlcNAcylation prevents its phosphorylation and deactivation, thereby inhibiting S1P-mediated contraction. a) MYTP1Δ expression sensitizes cells to S1P-mediated contraction. NIH3T3 cells stably expressing either MYPT1 or MYTP1Δ were transfected with RNAi to downregulate endogenous MYTP1. They were then treated with the indicated concentrations of S1P for 30 min. The contraction phenotype was visualized using bright-field microscopy. b) Quantitation of the data in (a). Results are the mean ± SEM of the relative culture plate area taken-up by cells in four randomly selected frames. Statistical significance was determined using a 2-way ANOVA test followed by Sidak's multiple comparisons test. c) MYPT1Δ is more readily phosphorylated upon low S1P signaling. NIH3T3 cells stably expressing either MYPT1 or MYTP1Δ were transfected with RNAi to downregulate endogenous MYTP1. They were then treated with S1P (100 nM) for the indicated lengths of time. MLC and MYPT1/MYPT1Δ phosphorylation were analyzed by Western blotting. d) Our model. When MYPT1 is O-GlcNAcylated it is more resistant to phosphorylation and deactivation, thus maintaining the brakes on contraction. When MYTP1 O-GlcNAcylation is lost, it is phosphorylated, resulting in MLC phosphorylation and contraction. e) Direct MYPT1 O-GlcNAcylation is largely responsible for the phenotype. NIH3T3 cells stably expressing either MYPT1 or MYTP1Δ were transfected with RNAi to downregulate endogenous MYTP1. MYTP1-expressing cells were then treated with either DMSO or 5SGlcNAc (200 μM) for 16 h. Cells under all three sets of conditions were then treated with the indicated concentrations of S1P for 30 min. The contraction phenotype was visualized using bright-field microscopy. f) Quantitation of the data in (e). Results are the mean ± SEM of the relative culture plate area taken-up by cells in four randomly selected frames. Statistical significance was determined using a 2-way ANOVA test followed by Sidak's multiple comparisons test.

Finally, we wanted to rule out the possibilities that deletion of the serine/threonine region of MYPT1 has an effect beyond inhibiting O-GlcNAcylation and/or that O-GlcNAc on another protein contributes to the observed contraction. If neither of these possibilities is true, we would predict that cells expressing MYPT1Δ would respond to S1P in the same way as cells expressing wild-type MYPT1 treated with 5SGlcNAc. Accordingly, we compared three different conditions: cells stably expressing MYPT1, cells stably expressing MYPT1 in the presence of 5SGlcNAc, and cells stably expressing MYPT1Δ. In all cases RNAi was used to remove the endogenous copy of MYPT1 from the NIH3T3 cells. Subsequent treatment of these populations of cells with S1P (0.05 - 5 μM) demonstrated that loss of MYPT1 O-GlcNAcylation in the serine/threonine region (i.e., MYPT1Δ) sensitized cells to the same extent as 5SGlcNAc treatment (Figure 6e & f). Importantly, cells expressing MYPT1 without 5SGlcNAc were again more resistant to S1P (Figure 6e & f). These data were recapitulated in a biological replicate, were the response of MYTP1Δ and MTYP1 plus 5SGlcNAc tracked closely together (Supplementary Figure 8). These data are consistent with our model that MYPT1 O-GlcNAcylation is directly responsible for regulating this signaling pathway and that this is the major modification event controlling this process (Supplementary Figure 9).

DISCUSSION

Taken together, these results strongly suggest that that MYPT1 O-GlcNAcylation functions as a nutrient sensor to regulate the sensitivity of fibroblasts to S1P-mediated contraction. At this time, we do not yet know the biological consequences of this regulation in more complex setting, but there is reason to believe that they could be numerous. In the case of fibroblasts, both S1P and Rho/ROCK signaling have been shown to play key roles in tissue fibrosis, particularly clinically important roles in pathological pulmonary fibrosis[50-52]. Additionally, S1P signaling in fibroblasts has been shown to increase wound healing, strikingly through the same receptor, S1PR2, that is responsible for our observed phenotype[53-56]. We speculate that in human diseases with elevated O-GlcNAc levels, particularly diabetes and cancer, that S1P signaling to MLC may be attenuated with detrimental consequences for fibroblast motility and differentiation. As initial support for this hypothesis, we have shown S1P-mediated contraction in patient-derived lung fibroblasts is also controlled by O-GlcNAcylation levels (Supplementary Figure 10). Furthermore, MYPT1 activity is critical for controlling smooth muscle contraction and therefore blood pressure. Several different GPCR agonists, including angiotensin, endothelin-1, S1P, epinephrine, and others activate the same Rho/ROCK pathway leading to MYPT1 phosphorylation and increased smooth muscle contraction[57-59]. Given our model where O-GlcNAcylation of MYTP1 acts downstream of ROCK, we hypothesize that this modification will control the sensitivity of smooth muscle cells to these various inputs, with potential implications in atherosclerosis and heart disease.

In summary, we present a biological model where O-GlcNAcylation of MYPT1 maintains its phosphatase activity by inhibiting the introduction of inactivating phosphorylation marks by ROCK1/2. This O-GlcNAcylation can then function in its well-established role as a sensor of the cellular environment and state to control the responsiveness of cells to contractile stimuli. In the past, the documented interaction between OGT and MYPT1 was thought to play only an adapter

function for OGT substrate selection[39], but we demonstrate here that O-GlcNAcylation of MYPT1 has its own important direct functions. We do not yet know the precise molecular mechanism by which O-GlcNAc inhibits MYPT1 phosphorylation. It could simply prevent ROCK/MYTP1 binding altogether or cause structural changes in MYTP1 that only prevent phosphorylation, and we are currently pursuing these possibilities. Additionally, we do not know the specific O-GlcNAc modification sites in the MYPT1 serine/threonine rich region that are most consequential. However, we believe that this will be very difficult to definitively determine. This region contains several stretches of multiple serines or threonines in a row, and OGT demonstrates the flexibility to heterogeneously modify such sequences, rendering single point-mutants unlikely to have large effects. We do plan to more accurately map the major general locations of MYTP1 O-GlcNAcylation within this 50 amino acid region in the future. Finally, our experiment comparing the effects of 5SGlcNAc treatment to MYTP1Δ expression cannot completely rule out some contribution of other O-GlcNAcylated proteins. Unfortunately, this "loss-of-modification" experiment is a general limitation of O-GlcNAc studies in cells, as to-date there are no robust methods for the site- or even protein-selective introduction of O-GlcNAcylation. However, we believe that the breadth of our experiments and heavy and dynamic nature of MYPT1 O-GlcNAcylation strongly support both our conclusions and the future exploration of these modifications in a variety of biological contexts.

METHODS

Methods and any associated references are available in the online version of the paper.

ACKNOWLEDGMENTS

The authors thank Prof. Amy Ryan (Firth) at the University of Southern California for the gift of the primary human fibroblasts. This research was supported by the American Cancer Society Research Scholar Grant (RSG-14-225-01-CCG to M.R.P.), the University of Southern California, the Anton Burg Foundation, and the National Institutes of Health (T32GM118289 for N.J.P). was supported by T32GM118289.

AUTHOR CONTRIBUTIONS

N.J.P., A.R.B., N.D. and M.R.P. designed experiments and interpreted data. N.J.P. and A.R.B carried out cellular phenotype and Western blotting experiments. N.J.P. generated stable cell lines and performed RNAi experiments. N.D. performed the analysis of MYPT1 O-GlcNAcylation levels and dynamics. N.J.P, A.R.B. and M.R.P. prepared the manuscript.

COMPETING FINANCIAL INTERESTS

The authors declare no competing financial interests.

ADDITIONAL INFORMATION

Supplementary information is available in the online version of the paper. Reprints and permissions information is available online at http://www.nature.com/reprints/index. html. Correspondence and requests for materials should be addressed to M.R.P.

REFERENCES

(1) Bond, M. R.; Hanover, J. A. A Little Sugar Goes a Long Way: the Cell Biology of O-GlcNAc. *J Cell Biol* **2015**, *208* (7), 869–880.

(2) Yang, X.; Qian, K. Protein O-GlcNAcylation: Emerging Mechanisms and Functions. *Nat Rev Mol Cell Biol* **2017**, *18* (7), 452–465.

(3) Zachara, N. E. Critical Observations That Shaped Our Understanding of the Function(S) of Intracellular Glycosylation (O-Glc NAc). *FEBS Lett* **2018**, *592* (23), 3950–3975.

(4) Vocadlo, D. J. O-GlcNAc Processing Enzymes: Catalytic Mechanisms, Substrate Specificity, and Enzyme Regulation. *Curr Opin Chem Biol* **2012**, *16* (5-6), 488–497.

(5) Levine, Z. G.; Walker, S. The Biochemistry of O-GlcNAc Transferase: Which Functions Make It Essential in Mammalian Cells? *Annu Rev Biochem* **2016**, *85* (1), 631–657.

(6) Joiner, C. M.; Li, H.; Jiang, J.; Walker, S. Structural Characterization of the O-GlcNAc Cycling Enzymes: Insights Into Substrate Recognition and Catalytic Mechanisms. *Curr. Opin. Struct. Biol.* **2019**, *56*, 97–106.

(7) Hart, G. W.; Slawson, C.; Ramirez-Correa, G.; Lagerlof, O. Cross Talk Between O-GlcNAcylation and Phosphorylation: Roles in Signaling, Transcription, and Chronic Disease. *Annu Rev Biochem* **2011**, *80*, 825–858.

(8) Wang, S.; Huang, X.; Sun, D.; Xin, X.; Pan, Q.; Peng, S.; Liang, Z.; Luo, C.; Yang, Y.; Jiang, H.; Huang, M.; Chai, W.; Ding, J.; Geng, M. Extensive Crosstalk Between O-GlcNAcylation and Phosphorylation Regulates Akt Signaling. *PLoS ONE* **2012**, *7* (5), e37427.

(9) Tarrant, M. K.; Rho, H.-S.; Xie, Z.; Jiang, Y. L.; Gross, C.; Culhane, J. C.; Yan, G.; Qian, J.; Ichikawa, Y.; Matsuoka, T.; Zachara, N.; Etzkorn, F. A.; Hart, G. W.; Jeong, J. S.; Blackshaw, S.; Zhu, H.; Cole, P. A. Regulation of CK2 by Phosphorylation and O-GlcNAcylation Revealed by Semisynthesis. *Nat Chem Biol* **2012**, *8* (3), 262–269.

(10) Rexach, J. E.; Clark, P. M.; Mason, D. E.; Neve, R. L.; Peters, E. C.; Hsieh-Wilson, L. C. Dynamic O-GlcNAc Modification Regulates CREB-Mediated Gene Expression and Memory Formation. *Nat Chem Biol* **2012**, *8* (3), 253–261.

(11) Shafi, R.; Iyer, S. P.; Ellies, L. G.; O'Donnell, N.; Marek, K. W.; Chui, D.; Hart, G. W.; Marth, J. D. The O-GlcNAc Transferase Gene Resides on the X Chromosome and Is Essential for Embryonic Stem Cell Viability and Mouse Ontogeny. *Proc Natl Acad Sci USA* **2000**, *97* (11), 5735–5739.

(12) Sinclair, D. A. R.; Syrzycka, M.; Macauley, M. S.; Rastgardani, T.; Komljenovic, I.; Vocadlo, D. J.; Brock, H. W.; Honda, B. M. Drosophila O-GlcNAc Transferase (OGT) Is Encoded by the Polycomb Group (PcG) Gene, Super Sex Combs (Sxc). *Proc Natl Acad Sci USA* **2009**, *106* (32), 13427–13432.

(13) Spiegel, S.; Milstien, S. Sphingosine-1-Phosphate: an Enigmatic Signalling Lipid. *Nat Rev Mol Cell Biol* **2003**, *4* (5), 397–407.

(14) Takabe, K.; Paugh, S. W.; Milstien, S.; Spiegel, S. "Inside-Out" Signaling of Sphingosine-1-Phosphate: Therapeutic Targets. *Pharmacol. Rev.* **2008**, *60* (2), 181–195.

(15) Mendelson, K.; Evans, T.; Hla, T. Sphingosine 1-Phosphate Signalling. *Development* **2013**, *141* (1), 5–9.

(16) Gonzalez-Cabrera, P. J.; Brown, S.; Studer, S. M.; Rosen, H. S1P Signaling: New Therapies and Opportunities. *F1000Prime Rep* **2014**, *6* (109), 109.

(17) Petrache, I.; Berdyshev, E. V. Ceramide Signaling and Metabolism in Pathophysiological States of the Lung. *Annu. Rev. Physiol.* **2016**, *78* (1), 463–480.

(18) Eto, M.; Kitazawa, T. Diversity and Plasticity in Signaling Pathways That Regulate Smooth Muscle Responsiveness: Paradigms and Paradoxes for the Myosin Phosphatase, the Master Regulator of Smooth Muscle Contraction. *J. Smooth Muscle Res.* **2017**, *53* (0), 1–19.

(19) Ogretmen, B. Sphingolipid Metabolism in Cancer Signalling and Therapy. *Nat Rev Cancer* **2017**, *18* (1), 33–50.

(20) Windh, R. T.; Lee, M. J.; Hla, T.; An, S.; Barr, A. J.; Manning, D. R. Differential Coupling of the Sphingosine 1-Phosphate Receptors Edg-1, Edg-3, and H218/Edg-5 to the G(I), G(Q), and G(12) Families of Heterotrimeric G Proteins. *J Biol Chem* **1999**, *274* (39), 27351–27358.

(21) Takuwa, Y. Subtype-Specific Differential Regulation of Rho Family G Proteins and Cell Migration by the Edg Family Sphingosine-1-Phosphate Receptors. *Biochim Biophys Acta* **2002**, *1582* (1-3), 112–120.

(22) Kluk, M. J.; Hla, T. Signaling of Sphingosine-1-Phosphate via the S1P/EDG-Family of G-Protein-Coupled Receptors. *Biochim Biophys Acta* **2002**, *1582* (1-3), 72–80.

(23) Riento, K.; Ridley, A. J. Rocks: Multifunctional Kinases in Cell Behaviour. *Nat Rev Mol Cell Biol* **2003**, *4* (6), 446–456.

(24) Amano, M.; Nakayama, M.; Kaibuchi, K. Rho-Kinase/ROCK: a Key Regulator of the Cytoskeleton and Cell Polarity. *Cytoskeleton (Hoboken)* **2010**, *67* (9), 545–554.

(25) Kureishi, Y.; Kobayashi, S.; Amano, M.; Kimura, K.; Kanaide, H.; Nakano, T.; Kaibuchi, K.; Ito, M. Rho-Associated Kinase Directly Induces Smooth Muscle Contraction Through Myosin Light Chain Phosphorylation. *J Biol Chem* **1997**, *272* (19), 12257–12260.

(26) Totsukawa, G.; Yamakita, Y.; Yamashiro, S.; Hartshorne, D. J.; Sasaki, Y.; Matsumura, F. Distinct Roles of ROCK (Rho-Kinase) and MLCK in Spatial Regulation of MLC Phosphorylation for Assembly of Stress Fibers and Focal Adhesions in 3T3 Fibroblasts. *The Journal of Cell Biology* **2000**, *150* (4), 797–806.

(27) Essler, M.; Retzer, M.; Ilchmann, H.; Linder, S.; Weber, P. C. Sphingosine 1-Phosphate Dynamically Regulates Myosin Light Chain Phosphatase Activity in Human Endothelial Cells. *Cellular Signalling* **2002**, *14* (7), 607–613.

(28) Koh, E.; Clair, T.; Hermansen, R.; Bandle, R. W.; Schiffmann, E.; Roberts, D. D.; Stracke, M. L. Sphingosine-1-Phosphate Initiates Rapid Retraction of Pseudopodia by Localized RhoA Activation. *Cellular Signalling* **2007**, *19* (6), 1328–1338.

(29) Feng, J.; Ito, M.; Ichikawa, K.; Isaka, N.; Nishikawa, M.; Hartshorne, D. J.; Nakano, T. Inhibitory Phosphorylation Site for Rho-Associated Kinase on Smooth Muscle Myosin Phosphatase. *J Biol Chem* **1999**, *274* (52), 37385–37390.

(30) Kawano, Y.; Fukata, Y.; Oshiro, N.; Amano, M.; Nakamura, T.; Ito, M.; Matsumura, F.; Inagaki, M.; Kaibuchi, K. Phosphorylation of Myosin-Binding Subunit (MBS) of Myosin Phosphatase by Rho-Kinase in Vivo. *The Journal of Cell Biology* **1999**, *147* (5), 1023–1038.

(31) Murányi, A.; Derkach, D.; Erdodi, F.; Kiss, A.; Ito, M.; Hartshorne, D. J. Phosphorylation of Thr695 and Thr850 on the Myosin Phosphatase Target Subunit: Inhibitory Effects and Occurrence in A7r5 Cells. *FEBS Lett* **2005**, *579* (29), 6611–6615.

(32) Wang, Y.; Zheng, X. R.; Riddick, N.; Bryden, M.; Baur, W.; Zhang, X.; Surks, H. K. ROCK Isoform Regulation of Myosin Phosphatase and Contractility in Vascular Smooth Muscle Cells. *Circ Res* **2009**, *104* (4), 531–540.

(33) Khasnis, M.; Nakatomi, A.; Gumpper, K.; Eto, M. Reconstituted Human Myosin Light Chain Phosphatase Reveals Distinct Roles of Two Inhibitory Phosphorylation Sites of the Regulatory Subunit, MYPT1. *Biochemistry* **2014**, *53* (16), 2701–2709.

(34) Heissler, S. M.; Sellers, J. R. Myosin Light Chains: Teaching Old Dogs New Tricks. *Bioarchitecture* **2014**, *4* (6), 169–188.

(35) Ito, M.; Nakano, T.; Erdodi, F.; Hartshorne, D. J. Myosin Phosphatase: Structure, Regulation and Function. *Mol Cell Biochem* **2004**, *259* (1-2), 197–209.

(36) Grassie, M. E.; Moffat, L. D.; Walsh, M. P.; MacDonald, J. A. The Myosin Phosphatase Targeting Protein (MYPT) Family: a Regulated Mechanism for Achieving Substrate Specificity of the Catalytic Subunit of Protein Phosphatase Type 1δ. *Arch Biochem Biophys* **2011**, *510* (2), 147–159.

(37) Takemoto, K.; Ishihara, S.; Mizutani, T.; Kawabata, K.; Haga, H. Compressive Stress Induces Dephosphorylation of the Myosin Regulatory Light Chain via RhoA Phosphorylation by the Adenylyl Cyclase/Protein Kinase a Signaling Pathway. *PLoS ONE* **2015**, *10* (3), e0117937.

(38) Hédou, J.; Cieniewski-Bernard, C.; Leroy, Y.; Michalski, J.-C.; Mounier, Y.; Bastide, B. O-Linked N-Acetylglucosaminylation Is Involved in the Ca2+ Activation Properties of Rat Skeletal Muscle. *J Biol Chem* **2007**, *282* (14), 10360–10369.

(39) Cheung, W. D.; Sakabe, K.; Housley, M. P.; Dias, W. B.; Hart, G. W. O-Linked Beta-N-Acetylglucosaminyltransferase Substrate Specificity Is Regulated by Myosin Phosphatase Targeting and Other Interacting Proteins. *J Biol Chem* **2008**, *283* (49), 33935–33941.

(40) Khidekel, N.; Arndt, S.; Lamarre-Vincent, N.; Lippert, A.; Poulin-Kerstien, K. G.; Ramakrishnan, B.; Qasba, P. K.; Hsieh-Wilson, L. C. A Chemoenzymatic Approach Toward the Rapid and Sensitive Detection of O-GlcNAc Posttranslational Modifications. *J Am Chem Soc* **2003**, *125* (52), 16162–16163.

(41) Clark, P. M.; Dweck, J. F.; Mason, D. E.; Hart, C. R.; Buck, S. B.; Peters, E. C.; Agnew, B. J.; Hsieh-Wilson, L. C. Direct in-Gel Fluorescence Detection and Cellular Imaging of O-GlcNAc-Modified Proteins. *J Am Chem Soc* **2008**, *130* (35), 11576–11577.

(42) Wang, S.; Yang, F.; Petyuk, V. A.; Shukla, A. K.; Monroe, M. E.; Gritsenko, M. A.; Rodland, K. D.; Smith, R. D.; Qian, W.-J.; Gong, C.-X.; Liu, T. Quantitative Proteomics Identifies Altered O-GlcNAcylation of Structural, Synaptic and Memory-Associated Proteins in Alzheimer's Disease. *J Pathol* **2017**, *243* (1), 78–88.

(43) Qin, K.; Zhu, Y.; Qin, W.; Gao, J.; Shao, X.; Wang, Y.-L.; Zhou, W.; Wang, C.; Chen, X. Quantitative Profiling of Protein O-GlcNAcylation Sites by an Isotope-Tagged Cleavable Linker. *ACS Chem Biol* **2018**, *13* (8), 1983–1989.

(44) Li, J.; Li, Z.; Duan, X.; Qin, K.; Dang, L.; Sun, S.; Cai, L.; Hsieh-Wilson, L. C.; Wu, L.; Yi, W. An Isotope-Coded Photocleavable Probe for Quantitative Profiling of Protein O-GlcNAcylation. *ACS Chem Biol* **2019**, *14* (1), 4–10.

(45) Ichikawa, K.; Hirano, K.; Ito, M.; Tanaka, J.; Nakano, T.; Hartshorne, D. J. Interactions and Properties of Smooth Muscle Myosin Phosphatase. *Biochemistry* **1996**, *35* (20), 6313–6320.

(46) Hirano, K.; Phan, B. C.; Hartshorne, D. J. Interactions of the Subunits of Smooth Muscle Myosin Phosphatase. *J Biol Chem* **1997**, *272* (6), 3683–3688.

(47) Tanaka, J.; Ito, M.; Feng, J.; Ichikawa, K.; Hamaguchi, T.; Nakamura, M.; Hartshorne, D. J.; Nakano, T. Interaction of Myosin Phosphatase Target Subunit 1 with the Catalytic Subunit of Type 1 Protein Phosphatase. *Biochemistry* **1998**, *37* (47), 16697–16703.

(48) Rexach, J. E.; Rogers, C. J.; Yu, S.-H.; Tao, J.; Sun, Y. E.; Hsieh-Wilson, L. C. Quantification of O-Glycosylation Stoichiometry and Dynamics Using Resolvable Mass Tags. *Nat Chem Biol* **2010**, *6* (9), 645–651.

(49) Darabedian, N.; Thompson, J. W.; Chuh, K. N.; Hsieh-Wilson, L. C.; Pratt, M. R. Optimization of Chemoenzymatic Mass Tagging by Strain-Promoted Cycloaddition (SPAAC) for the Determination of O-GlcNAc Stoichiometry by Western Blotting. *Biochemistry* **2018**, *57* (40), 5769–5774.

(50) Knipe, R. S.; Tager, A. M.; Liao, J. K. The Rho Kinases: Critical Mediators of Multiple Profibrotic Processes and Rational Targets for New Therapies for Pulmonary Fibrosis. *Pharmacol. Rev.* **2015**, *67* (1), 103–117.

(51) Wang, E.; He, X.; Zeng, M. The Role of S1P and the Related Signaling Pathway in the Development of Tissue Fibrosis. *Front Pharmacol* **2018**, *9*, 1504.

(52) Knipe, R. S.; Probst, C. K.; Lagares, D.; Franklin, A.; Spinney, J. J.; Brazee, P. L.; Grasberger, P.; Zhang, L.; Black, K. E.; Sakai, N.; Shea, B. S.; Liao, J. K.; Medoff, B. D.; Tager, A. M. The Rho Kinase Isoforms ROCK1 and ROCK2 Each Contribute to the Development of Experimental Pulmonary Fibrosis. *Am J Respir Cell Mol Biol* **2018**, *58* (4), 471–481.

(53) Serriere-Lanneau, V.; Teixeira-Clerc, F.; Li, L.; Schippers, M.; de Wries, W.; Julien, B.; Tran-Van-Nhieu, J.; Manin, S.; Poelstra, K.; Chun, J.; Carpentier, S.; Levade, T.; Mallat, A.; Lotersztajn, S. The Sphingosine 1-Phosphate Receptor S1P2 Triggers Hepatic Wound Healing. *FASEB J* **2007**, *21* (9), 2005–2013.

(54) Kawanabe, T.; Kawakami, T.; Yatomi, Y.; Shimada, S.; Soma, Y. Sphingosine 1-Phosphate Accelerates Wound Healing in Diabetic Mice. *J. Dermatol. Sci.* **2007**, *48* (1), 53–60.

(55) Vogler, R.; Sauer, B.; Kim, D.-S.; Schäfer-Korting, M.; Kleuser, B. Sphingosine-1-Phosphate and Its Potentially Paradoxical Effects on Critical Parameters of Cutaneous Wound Healing. *J Investig Dermatol* **2003**, *120* (4), 693–700.

(56) MD, K. N. F.-G.; MD, A. H. H.; Julie D Saba MD, P. Evidence-Based Surgical Hypothesis Normalization of Diabetic Wound Healing. *Surgery* **2010**, *147* (3), 446–449.

(57) SOMLYO, A. P.; SOMLYO, A. V. Ca2+ Sensitivity of Smooth Muscle and Nonmuscle Myosin II: Modulated by G Proteins, Kinases, and Myosin Phosphatase. *Physiol Rev* **2003**, *83* (4), 1325–1358.

(58) Grassie, M. E.; Sutherland, C.; Ulke-Lemée, A.; Chappellaz, M.; Kiss, E.; Walsh, M. P.; MacDonald, J. A. Cross-Talk Between Rho-Associated Kinase and Cyclic Nucleotide-Dependent Kinase Signaling Pathways in the Regulation of Smooth Muscle Myosin Light Chain Phosphatase. *J Biol Chem* **2012**, *287* (43), 36356–36369.

(59) Qiao, Y.-N.; He, W.-Q.; Chen, C.-P.; Zhang, C.-H.; Zhao, W.; Wang, P.; Zhang, L.; Wu, Y.-Z.; Yang, X.; Peng, Y.-J.; Gao, J.-M.; Kamm, K. E.; Stull, J. T.; Zhu, M.-S. Myosin Phosphatase Target Subunit 1 (MYPT1) Regulates the Contraction and Relaxation of Vascular Smooth Muscle and Maintains Blood Pressure. *J Biol Chem* **2014**, *289* (32), 22512–22523.